PHYSICAL REVIEW D, VOLUME 62, 014002

Penguin diagrams in the $\Delta I=1/2$ rule and ϵ'/ϵ with σ models

M. Harada*
Department of Physics, Nagoya University, Nagoya, 464-8602, Japan

Y. Y. Keum†
Theory Group, KEK, Tsukuba, Ibaraki 305-0801, Japan

Y. Kiyo,‡ T. Morozumi,§ T. Onogi,‖ and N. Yamada¶
Department of Physics, Hiroshima University, 1-3-1 Kagamiyama, Higashi Hiroshima-739-8526, Japan

(Received 5 October 1999; published 18 May 2000)

We study the correlation between ϵ'/ϵ and the $\Delta I=1/2$ rule in the frame-work of the nonlinear σ model including scalar mesons. Using this model we estimate the chiral corrections by resumming to all orders in chiral perturbation theory, the contribution of a class of diagrams within the factorization approximation. With these matrix elements and changing the scalar meson mass, we find that there is a correlation between ϵ'/ϵ and the $\Delta I=1/2$ amplitude. However, it is difficult to explain both ϵ'/ϵ and the $\Delta I=1/2$ amplitude simultaneously. In order to be compatible with ϵ'/ϵ, typically, about half of the $\Delta I=1/2$ amplitude can be explained at most. Our result suggests there may be a substantial nonfactorizable contribution to *CP* conserving $K\to\pi\pi$ amplitudes.

PACS number(s): 12.39.Fe, 14.40.Cs

I. INTRODUCTION

According to recent measurements of direct *CP* violation in $K\to\pi\pi$ decays, ϵ'/ϵ is $O(10^{-3})$ [1,2]. Theoretical prediction ranges between 10^{-4} and 10^{-3}. It strongly depends on the hadronic matrix elements of QCD [3] and the electroweak (EW) penguin operators [4–6].

An interesting possibility is suggested as an explanation for large $\epsilon'/\epsilon=O(10^{-3})$ in the standard model [7]. The authors argue that the mechanism which enhances the $\Delta I=1/2$ amplitude may also enhance ϵ'/ϵ and it naturally leads to the measured values. The enhancement comes from the Feynman diagram which includes the scalar σ meson as an intermediate state. The mechanism was found in the framework of the linear σ model [8,9]. Though the qualitative picture of the linear σ model may be correct, for a quantitative analysis, some improvement can be made. In the linear σ model employed in Ref. [9], the σ meson mass can be written in terms of the physical quantities F_K, F_π, M_K, and M_π and its mass is predicted to be about 900 MeV. SU(3) breaking ratio m_u/m_s is also determined by the same input and numerically it is around 1/30. The enhancement factor of a QCD penguin operator is written as $F_K/(3F_\pi-2F_K)=(M_\sigma\sigma^2-M_\pi^2)/(M_\sigma^2-M_K^2)\cdot(F_K^2/F_\pi^2)\simeq 2$. These relations and numbers are specific predictions of the linear σ model. Because the dynamical property of the linear σ model is not the same as that of QCD, these relations and numbers may be taken as semiquantitative [7].

In this paper, we study the matrix elements of the QCD and EW penguin operators with the nonlinear σ model including scalar mesons. The model is built with chiral symmetry as a guide. It is more general than the linear σ model and less dependent on dynamical assumption. The cost is that it has more parameters. They can be determined with the experimental measured quantities, i.e., decay width, mass spectrum, etc. Still σ meson mass is left as a free parameter because the spectroscopy of σ meson $f_0(400-1200)$ allows a wide range for the mass. (See Refs. [10–15] for scalar meson mass spectroscopy.) We study how QCD and EW penguin matrix elements depend on the mass of the σ meson.

Here we write a few words on the difference between our approach and the conventional treatment of the resonances in chiral perturbation theory (CHPT). CHPT is a systematic treatment, in the sense of the small momentum expansion, and describes low-energy processes involving pions and kaons. However, higher order terms in CHPT are of great importance if the threshold of the σ meson is near to kaon mass. Thus it is very interesting to explore the nonlinear σ model with scalar resonances in kaon decays. Correspondence between the nonlinear σ model with resonances and CHPT was well discussed in Refs. [16,17] at order of p^4 and the results indicate that the resonance contributions dominate the low-energy coupling constants in the strong part of the p^4 chiral Lagrangian. In our approach, we compute the full contribution of the σ meson to the factorizable part of QCD and EW penguin operators using the nonlinear σ model with scalar resonances, so that a certain class of higher order terms of $p^n(n>4)$ in momentum expansion is included. We show how these higher order terms contribute to observable kaon decays.

As a phenomenological application, we compute ϵ'/ϵ and the $\Delta I=1/2$ amplitude in the isospin limit. We use the Wilson coefficients for four-Fermi interaction at $\mu=0.8-1.2$ GeV in the next to leading log (NLL) approxima-

*Email address: harada@eken.phys.nagoya-u.ac.jp
†Email address: keum@ccthmail.kek.jp
‡Email address: kiyo@theo3.phys.sci.hiroshima-u.ac.jp
§Email address: morozumi@theo.phys.sci.hiroshima-u.ac.jp
‖Email address: onogi@theo.phys.sci.hiroshima-u.ac.jp
¶Email address: yamada@theo3.phys.sci.hiroshima-u.ac.jp

tion [18–20]. The four-Fermi operator is factorized into products of color singlet currents (or densities) and they are identified with those of the σ model [21]. The density $\times$ density type operators are enhanced for small strange quark mass by a factor of $(1/m_s)^2$. Therefore numerical values for the strange quark mass are important. As for the strange quark mass, we choose the range which is suggested by the QCD sum rule [22] and lattice simulations [23]. We also study the correlation between ϵ'/ϵ and the $\Delta I=1/2$ amplitude. This is done by varying the σ mass, strange quark mass m_s, and factorization scale μ. By studying the dependence of ϵ'/ϵ and the $\Delta I=1/2$ amplitude on the σ meson mass, we search for the range of the mass which may reproduce both ϵ'/ϵ and the $\Delta I=1/2$ amplitude.

The paper is organized as follows: In Sec. II, we summarize the outline of the computation ϵ'/ϵ and the $\Delta I=1/2$ amplitude. In Sec. III, we derive the matrix elements of penguin operators. In Sec. IV, numerical results of ϵ'/ϵ and $\Delta I=1/2$ are summarized. In Sec. V, we discuss the implication of our results. Some useful formulas are collected in the appendixes.

II. $\Delta I=1/2$ RULE AND ϵ'/ϵ IN THE STANDARD MODEL

In this section, we summarize our notations and show an outline of computation of ϵ'/ϵ and the $\Delta I=1/2$ amplitude. Some details of definitions of isospin amplitudes can be found in Appendix A. We start with the effective Hamiltonian for $\Delta S=1$ nonleptonic decays [18],

$$H_{\rm eff}=\frac{G_F}{\sqrt{2}}V_{ud}V_{us}^*\sum_{i=1}^{10}\{z_i+\tau y_i\}Q_i+\text{H.c.},\qquad(1)$$

where $\tau=-(V_{td}V_{ts}^*)/(V_{ud}V_{us}^*)$. The isospin amplitudes of $K\to\pi\pi$ are defined as $\langle I|H_{\rm eff}|K^0\rangle=ia_I\exp i\delta_I$, $\langle I|H_{\rm eff}|\overline{K^0}\rangle=-ia_I^*\exp(i\delta_I)$. ϵ' is expressed in terms of a_0 and a_2

$$\epsilon'=\frac{1}{\sqrt{2}}\frac{\text{Re}\,a_2}{\text{Re}\,a_0}\left(\frac{\text{Im}\,a_2}{\text{Re}\,a_2}-\frac{\text{Im}\,a_0}{\text{Re}\,a_0}\right)\exp\left\{i\left(\delta_2-\delta_0+\frac{\pi}{2}\right)\right\}.\qquad(2)$$

In the factorization approximation, a_I's are written as

$$\text{Re}\,a_I=\frac{G_F}{\sqrt{2}}\text{Re}\,V_{ud}V_{us}^*\sum_{i=1}^{5}\left[\left(z_{2i-1}+\frac{z_{2i}}{N_c}\right)\langle I|Q_{2i-1}|K^0\rangle+\left(z_{2i}+\frac{z_{2i-1}}{N_c}\right)\langle I|Q_{2i}|K^0\rangle\right]\frac{1}{i},\qquad(3)$$

$$\text{Im}\,a_I=-\frac{G_F}{\sqrt{2}}\text{Im}\,V_{td}V_{ts}^*\sum_{i=1}^{5}\left[\left(y_{2i-1}+\frac{y_{2i}}{N_c}\right)\langle I|Q_{2i-1}|K^0\rangle+\left(y_{2i}+\frac{y_{2i-1}}{N_c}\right)\langle I|Q_{2i}|K^0\rangle\right]\frac{1}{i},\qquad(4)$$

where the matrix elements $\langle I|Q_iK^0\rangle$ are defined in the large N_c limit. As we discuss in detail in the next section, we compute the hadronic matrix element in the large N_c limit; i.e., we factorize the four-Fermi operators into products of color singlet currents (densities). The currents (densities) are identified with those of the chiral Lagrangian. The factorization scale is chosen at 0.8-1.2 GeV, i.e., below charm quark mass m_c. In the factorization approximation, this choice is mandatory because above m_c, the real part of the Wilson coefficient of QCD penguin operators is zero and it is born below m_c due to the incomplete cancellation of the Glashow-Iliopoulos-Macroni (GIM) mechanism. Regarding Wilson coefficients, we use the NLL approximation [18–20] and compute them at the factorization scale. Combining the matrix elements with the Wilson coefficients, a_I's are given as

TABLE I. The matrix elements, where $X=i\sqrt{2}f(M_k^2-M_\pi^2)$. $\tilde{Y}_8$ and Y_6 are defined in the text.

	$\pi^0\pi^0$	$\vert\pi^+\rangle\times\vert\pi^-\rangle$	$\vert\pi^0\rangle\times\vert\pi^+\rangle$
Q_1	$-X$	0	$X/\sqrt{2}$
Q_2	0	X	$X/\sqrt{2}$
Q_3	0	0	0
Q_4	X	X	0
Q_5	0	0	0
Q_6	Y_6	Y_6	0
Q_7	$3X/2$	0	$-3X/2\sqrt{2}$
$\tilde{Q}_8$	0	$\tilde{Y}_8$	$\tilde{Y}_8/\sqrt{2}$
Q_9	$-3X/2$	0	$3X/2\sqrt{2}$
Q_{10}	$-X/2$	X	$X/\sqrt{2}$
Q_{11}	X	0	$X/\sqrt{2}$

$$\text{Re}\,a_0=\frac{G_F}{\sqrt{6}}\lambda\frac{X}{i}\left[2z_2+3z_4-z_1+3z_6\frac{Y_6}{X}\right],$$

$$\text{Re}\,a_2=\frac{G_F}{\sqrt{3}}\lambda\frac{X}{i}[z_1+z_2],$$

$$\text{Im}\,a_0=\frac{-\sqrt{3}G_F}{\sqrt{2}}\frac{X}{i}(A\lambda^2)^2\lambda\,\eta\left[y_4+\frac{y_7-y_9+y_{10}}{2}+y_6\frac{Y_6}{X}+\frac{2}{3}y_8\frac{\tilde{Y}_8-\frac{3}{4}Y_6}{X}\right],$$

$$\text{Im}\,a_2=\frac{-\sqrt{3}G_F}{2}\frac{X}{i}(A\lambda^2)^2\lambda\,\eta\left[-y_7+y_9+y_{10}+\frac{2}{3}y_8\frac{\tilde{Y}_8}{X}\right],\qquad(5)$$

where matrix elements are denoted by X, Y_6, and $\tilde{Y}_8$. X is the matrix element of current$\times$current type operators, Y_6 corresponds to the matrix element of a density$\times$density QCD penguin operator, and $\tilde{Y}_8$ is the matrix element of the EW penguin operator. Their derivation and precise definition will be given in the next section and are summarized in Tables I and II.

TABLE II. Contribution to isospin amplitudes.

	a_0	a_2
Q_1	$-\sqrt{\frac{1}{3}}X$	$\sqrt{\frac{2}{3}}X$
Q_2	$\frac{2}{\sqrt{3}}X$	$\sqrt{\frac{2}{3}}X$
Q_3	0	0
Q_4	$\sqrt{3}X$	0
Q_5	0	0
Q_6	$\sqrt{3}Y_6$	0
Q_7	$\frac{\sqrt{3}}{2}X$	$-\sqrt{\frac{3}{2}}X$
Q_8	$\frac{2}{\sqrt{3}}\tilde{Y}_8-\frac{\sqrt{3}}{2}Y_6$	$\sqrt{\frac{2}{3}}\tilde{Y}_8$
Q_9	$-\frac{\sqrt{3}}{2}X$	$\sqrt{\frac{3}{2}}X$
Q_{10}	$\frac{\sqrt{3}}{2}X$	$\sqrt{\frac{3}{2}}X$

III. NONLINEAR σ MODEL INCLUDING SCALAR MESONS AND THE MATRIX ELEMENTS OF QCD AND EW PENGUIN OPERATORS

The nonlinear σ model with higher resonances is studied in [16,17]. In $K\to\pi\pi$ decays, in the large N_c limit, the scalar meson may contribute to the matrix elements of density$\times$density type four-Fermi operators (Q_6,Q_8). For current$\times$current type four-Fermi interactions, the amplitude is proportional to the form factor of semileptonic decay, i.e., $f_+(M_K^2-M_\pi^2)+f_-M_\pi^2$. Because the form factors $f_\pm(q^2)$ near the soft-pion limit $(q^2=M_\pi^2)$ are important, vector meson contribution to the form factors is small and their effect can be safely neglected. Therefore we include only scalar mesons in the chiral Lagrangian:

$$\mathcal{L}=\frac{f^2}{4}\mathrm{Tr}\,\partial U\partial U^\dagger+B\,\mathrm{Tr}\,\mathcal{M}(U+U^\dagger)+\frac{g_1}{4}\mathrm{Tr}\,\partial U\partial U^\dagger\xi S\xi^\dagger +g_2\,\mathrm{Tr}\,\mathcal{M}(\xi S\xi+\xi^\dagger S\xi^\dagger)+\mathrm{Tr}(DSDS-M_\sigma^2S^2), \quad (6)$$

where $\mathcal{M}=\mathrm{diag}(m_u,m_d,m_s)$, $U=\exp(i2\pi/f)=\xi^2$, and S is a scalar nonet field,

$$S=\frac{1}{2}\begin{pmatrix}\sigma+\delta^0 & \sqrt{2}\delta^0 & \sqrt{2}\kappa^+\\ \sqrt{2}\delta^0 & \sigma-\delta^0 & \sqrt{2}\kappa^0\\ \sqrt{2}\kappa^- & \sqrt{2}\kappa^0 & \sqrt{2}\delta_{ss}\end{pmatrix}. \quad (7)$$

DS is covariant derivative and is defined by

$$D_\mu S=\partial_\mu S+i[\alpha_{\parallel\mu},S], \quad (8)$$

$$\alpha_{\parallel\mu}=\frac{\xi^\dagger\partial_\mu\xi+\xi\partial_\mu\xi^\dagger}{2i}=\frac{[\pi,\partial_\mu\pi]}{2if^2}+\cdots. \quad (9)$$

In the Lagrangian, the scalar mesons couple to pions through two terms denoted by g_1 and g_2. One is a coupling in the SU(3) limit and the other is a coupling with SU(3) breaking. The mass splitting term for the scalar nonets and isospin breaking effect are neglected. By shifting the scalar meson fields from their vacuum expectation value,

$$S\to S+\langle S\rangle,\quad \langle S\rangle=\frac{g_2}{M_\sigma^2}\mathcal{M}, \quad (10)$$

we obtain the mass formulas and decay constants [16]. They are given in Appendix B. The parameters in the chiral Lagrangian can be written in terms of physical quantities F_K, F_π, M_K, M_π, and quark masses $m_u(=m_d)$ and m_s:

$$B=\frac{2}{m_s(1-\Delta)}\left[\frac{(\Delta+1)M_\pi^2F_\pi^2}{8\Delta}-\frac{\Delta M_K^2F_K^2}{2(1+\Delta)}\right], \quad (11)$$

$$\frac{g_2^2}{M_\sigma^2}=\frac{2}{m_s^2(1-\Delta)}\left[-\frac{F_{\pi s}^2M_\pi^2}{4\Delta}+\frac{F_K^2M_K^2}{2(1+\Delta)}\right], \quad (12)$$

$$\frac{g_1g_2}{M_\sigma^2}=\frac{2(F_K^2-F_\pi^2)}{m_s(1-\Delta)}, \quad (13)$$

where $\Delta=m_u/m_s$. For computation of the weak matrix elements, we need strong interaction vertices. They can be found in Appendix C.

In our calculation using the Lagrangian Eq. (6), a certain class of the higher order terms in the CHPT are summed up due to the effect of the scalar resonance exchange. These are very important in the process $K\to\pi\pi$ if the σ meson mass is as light as the kaon mass, $M_\sigma\sim M_K$. Though systematic treatment of momentum expansion in the CHPT is lost, a class of the higher order terms in the CHPT are automatically summed up using Lagrangian of Eq. (6).

Now we turn to the matrix element of QCD and EW penguin operators. The explicit derivation is given for two density$\times$density type operators Q_6 and Q_8. Their definitions are

$$Q_6=-8\sum_{q=u,d,s}(\overline{s_L}q_R)(\overline{q_R}d_L), \quad (14)$$

$$Q_8=-12\sum_{q=u,d,s}(\overline{s_L}q_R)e_q(\overline{q_R}d_L)=\tilde{Q}_8-\frac{1}{2}Q_6, \quad (15)$$

$$\tilde{Q}_8=-8(\overline{s_L}u_R)(\overline{u_R}d_L), \quad (16)$$

where the subsidiary operator $\tilde{Q}_8$ is introduced. These operators can be written in terms of meson fields by identifying the quark bilinear as the corresponding density,

$$\overline{q_R^j}q_L^i=-BU_{ij}-g_2[\xi(S+\langle S\rangle)\xi]_{ij}. \quad (17)$$

After some algebra, we express Q_6 in terms of the meson fields,

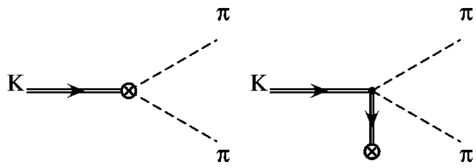

FIG. 1. Feynman diagrams for $T_{direct}+T_{tadpole}$.

$$Q_6=-8\Bigg[\frac{i}{\sqrt{2}}\frac{g_2^2(m_s-m_u)}{M_\sigma^2}\left(2B+\frac{g_2^2(m_s+m_u)}{M_\sigma^2}\right)\frac{K^0}{F_K} -\frac{i}{24\sqrt{2}}\frac{g_2^2(m_s-m_u)}{M_\sigma^2}\left(2B+\frac{g_2^2(m_s+m_u)}{M_\sigma^2}\right)\frac{K^0\pi^{0^2}}{F_KF_\pi^2} -\frac{ig_2}{2\sqrt{2}}\left\{\left(2B+g_2^2\frac{(m_s+m_u)}{M_\sigma^2}\right)\frac{\pi^0\kappa}{F_\pi} +\left(2B+\frac{g_2^2 2m_u}{M_\sigma^2}\right)\frac{\sigma K^0}{F_K}\right\}\Bigg]. \tag{18}$$

There are four diagrams which may contribute to $K^0\to\pi^0\pi^0$ amplitude Y_6. (See Feynman diagrams in Figs. 1–3) They are classified as follows.

(1) The diagram in which K^0 decays into $K^0\pi^0\pi^0$ through the strong vertex and subsequently K^0 vanishes into vacuum through the $Q_6(T_{\rm tadpole})$.

(2) The diagram in which K^0 directly decays into $2\pi^0(T_{\rm direct})$.

(3) The diagram in which K^0 is converted into σ and subsequently σ decays into $2\pi^0(T_{\sigma\text{-}pole})$.

(4) The diagram in which K decays into κ, π^0 through strong vertex and κ is converted into $\pi^0(T_{\kappa\text{-}pole})$.

The sum of the contribution is denoted by Y_6 and it can be simplified as

$$Y_6=\frac{i\sqrt{2}}{F_KF_\pi^2}\Bigg[-\frac{g_1g_2}{M_\sigma^2}\left\{\overline{B}_0\frac{M_K^2}{1-\delta_\pi^2}+\overline{B}\frac{M_K^2-2M_\pi^2}{1-\delta_k^2}\right\} +\frac{g_2^2}{M_\sigma^2}\Bigg\{\frac{4\overline{B}_0}{1-\delta_\pi^2}\left(m_s+m_u-\frac{(m_s-m_u)M_K^2}{2M_\sigma^2}\right)-\frac{8\overline{B}m_u}{1-\delta_k^2} -(m_s-m_u)\left(2\overline{B}_0+\overline{B}\left(1+\frac{1}{R^2}\right)\right)\Bigg\}-\frac{g_1g_2^3\overline{B}(m_s-m_u)^2}{2F_K^2M_\sigma^4} +\frac{g_2^4(m_s-m_u)^2}{M_\sigma^4}\Bigg], \tag{19}$$

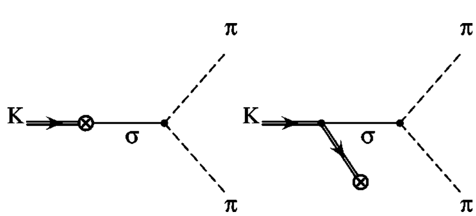

FIG. 2. Feynman diagrams for $T_{\sigma\text{-}pole}+T_{\sigma\text{-}tad}$.

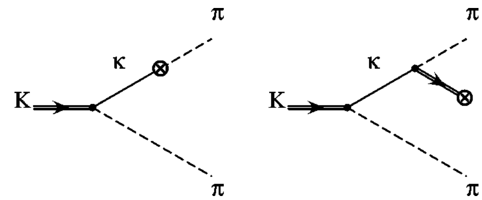

FIG. 3. Feynman diagrams for $T_{\kappa\text{-}pole}+T_{\kappa\text{-}tad}$.

where $R=F_K/F_\pi$ and $\delta_{K(\pi)}=M_{K(\pi)}/M_\sigma$. We also introduce the auxiliary quantities

$$\overline{B}=B+\frac{g_2^2(m_s+m_u)}{2M_\sigma^2},\quad \overline{B}_0=B+\frac{g_2^2m_u}{M_\sigma^2}. \tag{20}$$

They can be written in terms of physical quantities

$$\overline{B}=\frac{M_K^2F_K^2}{2m_s(1+\Delta)},\quad \overline{B}_0=\frac{M_\pi^2F_\pi^2}{4m_s\Delta}. \tag{21}$$

The matrix element of the EW penguin operator Q_8 is straightforward. Technically we split Q_6 from Q_8 so that we do not have to repeat the calculation of Q_6. The rest is called $\tilde{Q}_8$ and given by

$$\tilde{Q}_8=\left[ig_2\overline{B}_0\frac{\pi^-\kappa^+}{F_\pi}-i\frac{g_2\overline{B}_0(\overline{B}_0+\overline{B})}{\sqrt{2}}\frac{K^0\pi^+\pi^-}{F_KF_\pi^2}\right]+\cdots. \tag{22}$$

In the $K^0\to\pi^+\pi^-$ amplitude, there are two contributions to the hadron matrix element of $\tilde{Q}_8$, i.e., (a) κ-pole contribution and (b) direct contribution. The sum is called $\tilde{Y}_8$ and is given by

$$\tilde{Y}_8=-i\frac{3}{\sqrt{2}F_KF_\pi^2}\frac{\overline{B}_0}{M_\sigma^2-M_\pi^2}\left[g_1g_2M_K^2-2g_2^2\left\{(m_s+3\overline{m}) -(m_s-\overline{m})\frac{M_K^2-M_\pi^2}{M_\sigma^2}\right\}\right]+i6\sqrt{2}\frac{1}{F_KF_\pi^2}\overline{B}_0(\overline{B}+\overline{B}_0). \tag{23}$$

Keeping leading terms of $1/M_\sigma$ the matrix elements $Y_6,\tilde{Y}_8$ reduce to the well-known results $Y_6^0,\tilde{Y}_8^0$ [24], which correspond to those in the leading order of momentum expansion and in the large N_c limit:

$$Y_6^0=-4\sqrt{2}i(F_K-F_\pi)\left(\frac{M_K^2}{m_s+m_u}\right)^2,$$
$$\tilde{Y}_8^0=3\sqrt{2}iF_\pi\left(\frac{M_K^2}{m_s+m_u}\right)^2. \tag{24}$$

This approximation is valid only when $M_K\ll M_\sigma$. In the next section we will show how the values of the matrix elements of the density×density operators are different from $Y_6^0,\tilde{Y}_8^0$ numerically.

TABLE III. Bag factor.

$\Delta=1/20$	M_σ (GeV)	0.55	0.6	0.7	0.8	0.9	1.0
	$B_6^{1/2}$	5.27	3.29	2.22	1.84	1.64	1.52
	$B_8^{3/2}$	0.70	0.73	0.77	0.79	0.81	0.82
$\Delta=1/25$	M_σ (GeV)	0.55	0.6	0.7	0.8	0.9	1.0
	$B_6^{1/2}$	4.81	3.06	2.12	1.78	1.61	1.50
	$B_8^{3/2}$	0.90	0.93	0.96	0.99	1.00	1.01
$\Delta=1/30$	M_σ (GeV)	0.55	0.6	0.7	0.8	0.9	1.0
	$B_6^{1/2}$	4.48	2.90	2.05	1.75	1.60	1.51
	$B_8^{3/2}$	1.13	1.15	1.17	1.19	1.20	1.21

The matrix elements of the other current×current operators $Q_i(i\neq 6,8)$ are also shown in Tables I and II, and are expressed by a single amplitude X:

$$X=i\sqrt{2}f(M_K^2-M_\pi^2). \tag{25}$$

IV. NUMERICAL RESULTS

In this section, we first estimate the hadronic parameters $B_{6,8}$ corresponding to the matrix element Q_6 and Q_8 in the factorization approximation. We compare our results with those from the linear σ model. As an application, we also compute ϵ'/ϵ and $\mathrm{Re}\, a_0$,$\mathrm{Re}\, a_2$. This is done in the isospin limit.

The conventional bag factors $B_6^{1/2}$,$B_8^{3/2}$, as they are often referred to are defined by the following equation in our notation:

$$B_6^{1/2}=\frac{Y_6}{Y_6^0},\quad B_8^{3/2}=\frac{2\tilde{Y}_8-X}{2\tilde{Y}_8^0-X}. \tag{26}$$

As explained in Sec. III, using M_π, M_K, F_π, F_K as inputs, our model can be described by three free parameters in the Lagrangian M_σ, m_s, $\Delta=m_u/m_s$ and another parameter μ in the matching process which is the factorization scale.

We find that our model predicts that the factorizable part of $B_6^{1/2}$ ranges around 1.6–3.0 depending on the σ meson mass M_σ. The quark mass dependence is not significant. On the other hand, $B_8^{3/2}$ ranges around 0.7–1.1 depending on Δ. We varied Δ in the range of $1/20-1/30$ and smaller Δ gives a larger value of $B_8^{3/2}$. M_σ dependence is negligible for $B_8^{3/2}$. The numerical value is given in Table III.

Let us now compare our results with those from the linear σ model [9]. The factorizable bag factors are given by the following equations:

$$B_6^{1/2}=\frac{F_K}{3F_\pi-2F_K}\sim 2, \tag{27}$$

$$B_8^{3/2}\simeq\frac{F_K}{F_\pi}\sim 1.2. \tag{28}$$

Because there are only four parameters in the linear σ model Lagrangian, after using $M_{\pi,K}$,$F_{\pi,K}$ there are no free parameters left, so that the model predicts $\Delta=1/30$ and $M_\sigma\sim 0.9$ GeV.

From Table III we find that $B_8^{3/2}$ from our model with $\Delta=1/30$ and that from the linear σ model are consistent. It can be seen that the factorizable part of $B_6^{1/2}$ for $M_\sigma=0.9$ GeV is around 1.5, which is smaller than the linear σ model result.

Next we apply our result to ϵ'/ϵ and $\mathrm{Re}\, a_0$,$\mathrm{Re}\, a_2$. For numerical computation of ϵ'/ϵ, we use the experimental values for $\mathrm{Re}\, a_I$.

We have calculated the next to leading order Wilson coefficients in the naive dimensional regularization (NDR) scheme. We could reproduce the numerical values tabulated in Ref. [18] to a good extent. We chose the following values for the computation: $m_t=165.00$ GeV, $m_W=80.20$ GeV, $m_b=4.40$ GeV, $m_c=1.30$ GeV, $1/\alpha_{\mathrm{QED}}=129.0$, $\sin^2(\theta_W)=0.230$, $\Lambda_{\mathrm{QCD}}^{(5)}=0.226$ GeV, $\Lambda_{\mathrm{QCD}}^{(4)}=0.325$ GeV, $\alpha^{\overline{\mathrm{MS}}}(m_Z)^{(5)}=0.11799$. We list the Wilson coefficients z_i,y_i at scales $\mu=1.2, 1.0, 0.8$ GeV in Table IV. In this calculation, we used the anomalous dimensions at the NLO by Buras *et al.*

As was explained in Sec. II, in the leading order in the large N_c expansion, $\mathrm{Re}\, a_I$,$\mathrm{Im}\, a_I$ are obtained by multiplying Wilson coefficients $z_i(\mu)$,$y_i(\mu)$ with the matrix elements of $Q_1(\mu),\ldots,Q_{10}(\mu)$ in our model, where μ is the factorization scale which is assumed to be 0.8–1.2 GeV.

Here we should make one point about the quark mass. In the large N_c limit, we approximate the matrix elements with the $Q_6(\mu)$ operator by the product of matrix elements with scalar quark operator at scale μ. Using the PCAC (partial conservation of axial vector current) relation, we then convert them to $F_K M_K^2/m_s(\mu)$. Here, the scale of the strange quark mass should be the same scale μ. Therefore, when we substitute the mass parameter m_s in our final result, we should run the quark mass to the factorization scale $\mu=0.8, 1.0, 1.2$ GeV. For example, $m_s(2\text{ GeV})=80-120$ MeV corresponds to $m_s(0.8\text{ GeV})=136-204$ MeV.

Figure 4 shows the dependence of η from our model on the scalar resonance mass M_σ. Here, we take $m_s^{\overline{\mathrm{MS}}}(2\text{ GeV})=80{,}120{,}180$ MeV, which cover the recent QCD calculations [22,23], and the scale μ is chosen to be 0.8 GeV. Upper and lower lines correspond to the maximum and minimum values of ϵ'/ϵ, respectively. We find that when M_σ is larger

TABLE IV. List of Wilson coefficients y_i, z_i.

Wilson coeff.	$\mu = 80.2$ GeV	$\mu = 1.2$ GeV	$\mu = 1.0$ GeV	$\mu = 0.8$ GeV
y_1	0.0	0.0	0.0	0.0
y_2	0.0	0.0	0.0	0.0
y_3	0.0014715	0.03058	0.03335	0.03722
y_4	−0.0019375	−0.05871	−0.05884	−0.05844
y_5	0.0006458	0.00311	−0.00168	−0.01384
y_6	−0.0019375	−0.09797	−0.11672	−0.16226
y_7/α_{QED}	0.1262367	−0.03714	−0.03822	−0.04038
y_8/α_{QED}	0.0	0.14352	0.17174	0.23136
y_9/α_{QED}	−1.0606455	−1.46549	−1.54058	−1.69377
y_{10}/α_{QED}	0.9	0.57829	0.68795	0.89882
z_1	0.0526643	−0.45108	−0.52381	−0.64505
z_2	0.9812457	1.23913	1.28816	1.37464
z_3	0.0	0.00674	0.01353	0.03059
z_4	0.0	−0.01980	−0.03704	−0.07439
z_5	0.0	0.00569	0.00784	0.00844
z_6	0.0	−0.01950	−0.03698	−0.08023
z_7/α_{QED}	0.0	0.00940	0.01249	0.01989
z_8/α_{QED}	0.0	0.00349	0.01551	0.04725
z_9/α_{QED}	0.0	0.01127	0.02019	0.03993
z_{10}/α_{QED}	0.0	−0.00219	−0.00893	−0.02287

than 0.8 GeV in order for η to lie within 0.27–0.52, which is favored by other measurements of Cabibbo-Kobayashi-Masukawa (CKM) parameters, $m_s^{\overline{\rm MS}}(2\ {\rm GeV})$ should take a rather small value 0.09–0.12 GeV. These values are consistent with recent lattice QCD calculations [23] but smaller compared with QCD sum rule results [22]. On the other hand, as M_σ becomes smaller the Q_6 amplitude is enhanced; in order for η to lie within 0.27–0.52, the larger value of $m_s^{\overline{\rm MS}}(2\ {\rm GeV})$ is preferred.

Finally, in Fig. 5, we show the correlation of $a_0/a_0^{\rm exp}$ and ϵ'/ϵ by changing the scalar meson mass from 0.6 to 1 GeV. We take three different values of $m_s^{\overline{\rm MS}}(2\ {\rm GeV})$, which are 80, 100, and 120 MeV. We take three values for the factorization scale μ, which are 0.8, 1.0, and 1.2 GeV. We used the experimental values of Re a_I for the numerical analysis of ϵ'/ϵ. The *CP* violation parameter η is chosen to be 0.3 in the figure. The shaded region is the experimental data from KTeV and NA48 for ϵ'/ϵ at the 2-σ confidence level.

We find that ϵ'/ϵ can be easily explained in our model by a suitable choice of the parameters. Typical values of M_σ and $m_s^{\overline{\rm MS}}(2\ {\rm GeV})$ are around 0.8 GeV and around 120 MeV, respectively, almost independent of the factorization scale μ.

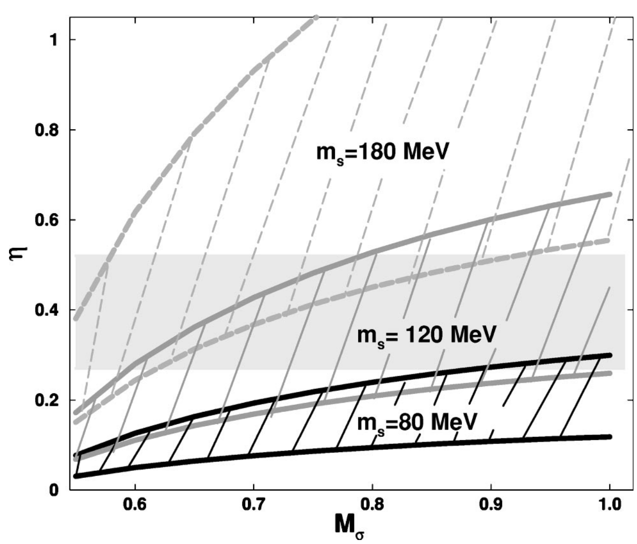

FIG. 4. Allowed regions for M_σ-η from ϵ'/ϵ data at 2-σ confidence level. They are shown for three different values for the strange quark mass, i.e., $m_s(2\ {\rm GeV}) = 80,\ 120,\ 180$ MeV.

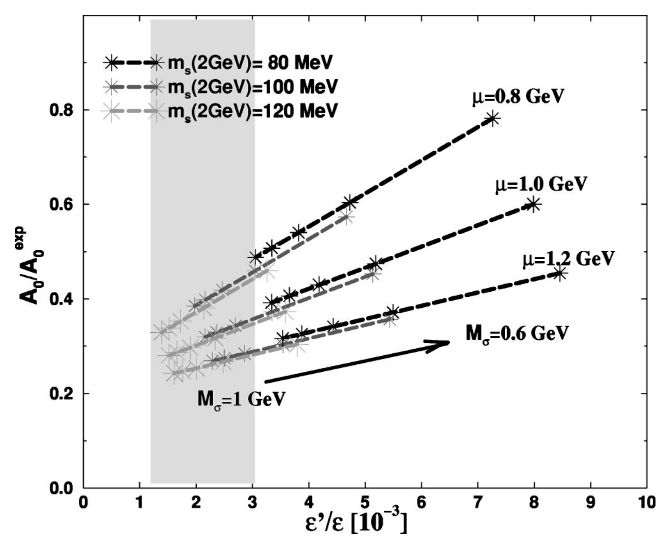

FIG. 5. Correlation of a_0 and ϵ'/ϵ. The stars on the lines correspond to $M_\sigma = 0.6$, 0.7, 0.8, 0.9, 1.0 GeV, $m_s(2\ {\rm GeV}) = 80,\ 100,\ 120$ MeV at factorization scale $\mu = 0.8, 1.0, 1.2$ GeV.

On the other hand, $\mathrm{Re}\, a_0$ in our model are smaller than experiment. We find that it is quite sensitive to the factorization scale μ, and as μ gets smaller, $\mathrm{Re}\, a_0$ becomes larger towards the experimental value. For $\mu=0.8$ GeV, a_0/a_0^{exp} is around 0.5–0.6.

The sensitivity of the a_0 amplitude on μ can be understood as follows. The Wilson coefficient $z_6(\mu)$ vanishes when the GIM cancellation between the charm penguin and the up penguin loop is exact. In our calculation, since we take the modified minimal subtraction ($\overline{\mathrm{MS}}$) scheme, the cancellation is exact above the charm threshold. Therefore, $z_6(\mu)$ takes nonzero value only when $\mu<m_c$. Since the factorization scale is very close to the charm threshold, the result of $z_6(\mu)$ changes quite a lot.

In contrast, the Wilson coefficient $y_6(\mu)$ vanishes when the GIM cancellation between the top penguin charm penguin loop is exact. Since the top decouples already below M_W, this cancellation is completely violated and $y_6(\mu)$ takes nonzero value from the start and keeps growing all the way down to the factorization scale. Since $\log(M_W/1.2\ \mathrm{GeV})$ and $\log(M_W/0.8\ \mathrm{GeV})$ are almost identical, $y_6(\mu)$ is not so sensitive to the factorization scale. Regarding $\mathrm{Re}\, a_2$, our result is about 1.5 times larger than the experimental value.

V. SUMMARY AND DISCUSSION

In this paper, we study the correlation of the $\Delta I=1/2$ amplitude and ϵ'/ϵ in the framework of the nonlinear σ model including the scalar mesons. We have calculated the matrix elements of the QCD and EW penguin operators using that model and within the factorization approximation.

We cannot find the scalar meson mass region which is compatible with both ϵ'/ϵ and the $\Delta I=1/2$ amplitude simultaneously. The reason is as follows. We can read from Fig. 5 that the maximum allowed value for $(\epsilon'/\epsilon)/\eta$ is about 0.01. The bag factor $B_6^{1/2}$ required for ϵ'/ϵ is at most 2–3, which corresponds to $M_{\sigma min}\simeq 0.6$–0.7 GeV. In the range of the scalar meson mass, about *half* of the $\Delta I=1/2$ amplitude may be explained. Therefore, if we impose the ϵ'/ϵ constraint, we cannot explain the whole $\Delta I=1/2$ amplitude. Moreover, ϵ'/ϵ is rather stable for the change of the factorization scale. This suggests that the prediction of ϵ'/ϵ may be more reliable. Though there is strong correlation between the $\Delta I=1/2$ amplitude and ϵ'/ϵ, we conclude that the understanding of the $\Delta I=1/2$ rule may not be complete.

Finally, we argue what kind of effects may remedy the problem. Because QCD penguin operator Q_6 is born just below m_c, the coefficient is not stable about the change of the factorization scale around 1 GeV. In the scheme, in which GIM cancellation is incomplete above $\mu\geqslant m_c$, the leading order results of the Wilson coefficient of Q_6 become larger by a factor of 2 [24]. This effect was not incorporated in the Wilson coefficients of the NLL approximation employed here. Therefore the same effect may further enhance the Wilson coefficient of Q_6 used in our analysis. We also note that the real part of the $\Delta I=3/2$ amplitude is larger by a factor of 1.5 than the experimental value. This may tell us that there is some suppression (enhancement) coming from the low-energy evolution (pion loops) for *CP*-conserving $\Delta I=3/2\,(\Delta I=1/2)$ amplitudes [25–29]. A plausible explanation is that the nonfactorizable contributions are very large. Including these effects may help for the entire understanding of both ϵ'/ϵ and the $\Delta I=1/2$ rule.

ACKNOWLEDGMENTS

We would like to thank T. Yamanaka, C. S. Lim, and U. Nierste for fruitful discussion and comments. Y.-Y.K. is grateful to M. Kobayashi for his encouragement. He would like to thank C. D. Lu for his hospitality during his stay at Hiroshima University. His work is supported by the Grant-in Aid for Scientific Research from the Ministry of Education, Science and Culture, Japan. The Work of T.M. is supported by the Grant-in Aid for Scientific Research (Physics of *CP* violation) from the Ministry of Education, Science and Culture, Japan.

APPENDIX A: $\Delta I=1/2$ RULE

Here we summarize isospin amplitudes

$$\Gamma[K_s\to\pi^0\pi^0]=Br(K_s\to\pi^0\pi^0)\times 1/\tau_s, \tag{A1}$$

$$\Gamma[K_s\to\pi^+\pi^-]=Br(K_s\to\pi^+\pi^-)\times 1/\tau_s, \tag{A2}$$

$$\Gamma[K^+\to\pi^0\pi^+]=Br(K^+\to\pi^0\pi^+)\times 1/\tau_+, \tag{A3}$$

where

$$\tau_s=(0.8927\pm0.0009)10^{-10}\ \ \mathrm{sec}, \tag{A4}$$

$$\tau_+=(1.2386\pm0.0024)10^{-8}\ \ \mathrm{sec}, \tag{A5}$$

$$\frac{1}{\tau_+}=5.3142\times10^{-14}\ \ \mathrm{MeV}, \tag{A6}$$

$$Br(K_s\to\pi^0\pi^0)=31.39\pm0.28\%, \tag{A7}$$

$$Br(K_s\to\pi^+\pi^-)=68.61\pm0.28\%, \tag{A8}$$

$$Br(K^+\to\pi^0\pi^+)=21.16\pm0.14\%, \tag{A9}$$

$$|I=0\rangle=\sqrt{\frac{1}{3}}|\pi^0\pi^0\rangle+\sqrt{\frac{2}{3}}|\pi^+\pi^-\rangle, \tag{A10}$$

$$|I=2,I_3=0\rangle=-\sqrt{\frac{2}{3}}|\pi^0\pi^0\rangle+\sqrt{\frac{1}{3}}|\pi^+\pi^-\rangle, \tag{A11}$$

$$|I=2,I_3=1\rangle=|\pi^0\pi^+\rangle, \tag{A12}$$

where $|\pi^+\pi^-\rangle$ and $|\pi^0\pi^+\rangle$ are the symmetrized states defined as

$$|\pi^+\pi^-\rangle=(|\pi^+\rangle\times|\pi^-\rangle+|\pi^-\rangle\times|\pi^+\rangle)/\sqrt{2}, \tag{A13}$$

$$|\pi^+\pi^0\rangle=(|\pi^+\rangle\times|\pi^0\rangle+|\pi^0\rangle\times|\pi^+\rangle)/\sqrt{2}. \tag{A14}$$

We can write the decay rates in terms of the isospin amplitudes:

$$\langle \pi^0\pi^0|H_w|K_s\rangle = i\sqrt{2}\left\{ \sqrt{\frac{1}{3}}\,\mathrm{Re}\,a_0 \exp i\,\delta_0 - \sqrt{\frac{2}{3}}\,\mathrm{Re}\,a_2 \exp i\,\delta_2 \right\}, \tag{A15}$$

$$\langle \pi^+\pi^-|H_w|K_s\rangle = i\sqrt{2}\left\{ \sqrt{\frac{2}{3}}\,\mathrm{Re}\,a_0 \exp i\,\delta_0 + \sqrt{\frac{1}{3}}\,\mathrm{Re}\,a_2 \exp i\,\delta_2 \right\}, \tag{A16}$$

$$\langle \pi^+\pi^0|H_w|K^+\rangle = i\sqrt{\frac{3}{2}}\,a_2, \tag{A17}$$

where $i a_I \exp(i\delta_I) = \langle I|H_w|K^0\rangle$, $I=0,2$, and $|K_s\rangle \simeq 1/\sqrt{2}(|K_0\rangle - |\overline{K_0}\rangle)$. With the definition, we can write

$$\Gamma(K_s\to\pi^0\pi^0) = P\,\frac{2}{3}\,|\mathrm{Re}\,a_0 \exp i\,\delta_0 - \sqrt{2}\,\mathrm{Re}\,a_2 \exp i\,\delta_2|^2\frac{1}{2}, \tag{A18}$$

$$\Gamma(K_s\to\pi^+\pi^-) = P\,\frac{2}{3}\,|\sqrt{2}\,\mathrm{Re}\,a_0 \exp i\,\delta_0 + \mathrm{Re}\,a_2 \exp i\,\delta_2|^2\frac{1}{2}, \tag{A19}$$

$$\Gamma(K^+\to\pi^0\pi^+) = P\,\frac{3}{4}\,\mathrm{Re}\,a_0^2, \tag{A20}$$

where imaginary parts are neglected. P is a phase space factor of two body decay and is defined as:

$$P = \frac{1}{16\pi M_K}\sqrt{1-4M_\pi^2/M_k^2} \tag{A21}$$

$$= 3.34919\times 10^{-5}\quad(\mathrm{MeV}^1). \tag{A22}$$

Here we use $M_{K^+} = 493.677\,\mathrm{MeV}$ and $\overline{M}_\pi = (M_{\pi^0} + M_{\pi^+})/2 = 137.273\,\mathrm{MeV}$. With these definitions, we obtain

$$\frac{Br(K^+\to\pi^0\pi^+)}{Br(K_s\to\pi^0\pi^0)+Br(K_s\to\pi^+\pi^-)}\,\frac{\tau_s}{\tau_+} = \frac{3}{4}\,\frac{\mathrm{Re}\,a_2^2}{\mathrm{Re}\,a_2^2+\mathrm{Re}\,a_0^2}. \tag{A23}$$

We can extract the following ratio and values for a_0 and a_2:

$$\frac{\mathrm{Re}\,a_0}{\mathrm{Re}\,a_2} = 22.15, \tag{A24}$$

$$\mathrm{Re}\,a_2 = 2.114\times 10^{-5}\quad(\mathrm{MeV}), \tag{A25}$$

$$\mathrm{Re}\,a_0 = 4.686\times 10^{-4}\quad(\mathrm{MeV}). \tag{A26}$$

APPENDIX B: DECAY CONSTANTS, MASS FORMULAS

In this appendix, we collect the formulas for the decay constants and masses which can be derived using Eq. (6).

$$M_\pi^2 = \frac{1}{F_\pi^2}\left[4Bm_u + 4\,\frac{g_2^2 m_u^2}{M_\sigma^2}\right], \tag{B1}$$

$$M_K^2 = \frac{1}{F_K^2}\left[2B(m_s+m_u) + \frac{g_2^2(m_s+m_u)^2}{M_\sigma^2}\right], \tag{B2}$$

$$F_\pi = \frac{f}{\sqrt{Z_\pi}}\left[1+\frac{g_1 g_2 m_u}{M_\sigma^2 f^2}\right], \tag{B3}$$

$$F_K = \frac{f}{\sqrt{Z_K}}\left[1+\frac{g_1 g_2(m_u+m_s)}{2M_\sigma^2 f^2}\right], \tag{B4}$$

$$Z_\pi = 1+\frac{g_1 g_2 m_u}{M_\sigma^2 f^2}, \tag{B5}$$

$$Z_K = 1+\frac{g_1 g_2 (m_u+m_s)}{2M_\sigma^2 f^2}, \tag{B6}$$

where Z_π and Z_K are wave function renormalization constants, F_π is 92.42 MeV.

APPENDIX C: LAGRANGIAN

Here we record the part of the Lagrangian which is relevant for calculation.

$$\mathcal{L}_{4\pi} = -\frac{\pi^2\partial K^0\partial\overline{K}^0}{12F_\pi^2} - \frac{K^0\overline{K}^0\partial{\pi^0}^2}{12F_K^2} + \frac{\pi^0\partial\pi^0(K^0\partial\overline{K}^0+\overline{K}^0\partial K^0)}{24}\left(\frac{1}{F_K^2}+\frac{1}{F_\pi^2}\right) + \frac{{\pi^0}^2K^0\overline{K}^0}{12F_\pi^2F_K^2}\left(F_\pi^2M_\pi^2+F_K^2M_K^2-\frac{3g_2^2(m_s-m_u)^2}{4M_\sigma^2}\right), \tag{C1}$$

$$\mathcal{L}_{s\pi\pi} = \frac{g_1}{4}\left[\sigma\left(\frac{(\partial\pi^0)^2}{F_\pi^2}+\frac{\partial K^0\partial\overline{K}^0}{F_K^2}\right) - \left(\overline{\kappa}^0\frac{\partial\pi^0\partial K^0}{F_\pi F_K}+\mathrm{H.c.}\right)\right] - g_2\left[\sigma\left(\frac{(\pi^0)^2}{F_\pi^2}m_u + \frac{K^0\overline{K}^0}{F_K^2}\left(\frac{m_u+m_s}{2}\right)\right) - \left(\overline{\kappa}^0\frac{\pi^0}{F_\pi}\frac{K^0}{F_K}\left(\frac{3m_u+m_s}{4}\right)+\mathrm{H.c.}\right)\right] + \delta\mathcal{L}_{s\pi\pi} + \delta\mathcal{L}_{4\pi}, \tag{C2}$$

where $\delta\mathcal{L}_{s\pi\pi}$ and $\delta\mathcal{L}_{4\pi}$ come from the covariant derivative term. [See Eq. (8) and Eq. (9).] Their explicit forms are

$$\delta\mathcal{L}_{s\pi\pi}=\frac{g_2(m_s-m_u)}{M_\sigma^2 4F_K F_\pi}[\partial\overline{\kappa}^0(K\overleftrightarrow{\partial}\pi^0)+\text{H.c.}], \tag{C3}$$

$$\delta\mathcal{L}_{4\pi}=\frac{g_2^2(m_s-m_u)^2}{16M_\sigma^4F_K^2F_\pi^2}[K^0\overleftrightarrow{\partial}\pi^0)(\overline{K}^0\overleftrightarrow{\partial}\pi^0)]. \tag{C4}$$

APPENDIX D: THE MATRIX ELEMENT OF Q_6

We give the derivation of the matrix element of Q_6

$$Y_6=T_{\text{tadpole}}+T_{\text{direct}}+T_{\sigma^-\text{pole}}+T_{\sigma^-\text{tad}}+T_{\kappa^-\text{pole}}+T_{\kappa^-\text{tad}}. \tag{D1}$$

The explicit expression of the parts of Eq. (19) is given by

$$\begin{aligned}T_{\text{tadpole}}+T_{\text{direct}}=&-\sqrt{2}i\frac{g_2^2}{M_\sigma^2F_K}(m_s-m_u)\overline{B}\left\{\frac{1}{F_K^2}+\frac{1}{F_\pi^2}\right.\\&-\frac{g_2^2(m_s-m_u)^2}{M^4F_K^2F_\pi^2}-\frac{g_2^2(m_s-m_u)^2}{F_K^2F_\pi^2M_\sigma^2M_K^2}\\&\left.+\frac{g_2^2(m_s-m_u)^2M_\pi^2}{F_K^2F_\pi^2M_\sigma^4M_K^2}\right\},\end{aligned}$$

$$\begin{aligned}T_{\sigma^-\text{pole}}+T_{\sigma^-\text{tad}}=&\frac{i\sqrt{2}\overline{B}}{F_KF_\pi^2(M_K^2-M_\sigma^2)}\{-g_1g_2(2M_\pi^2-M_K^2)\\&+8g_2^2m_u\},\end{aligned}$$

$$\begin{aligned}T_{\kappa^-\text{pole}}+T_{\kappa^-\text{tad}}=&\frac{i\sqrt{2}\overline{B}}{F_KF_\pi^2(M_\sigma^2-M_\pi^2)}\\&\times\left\{1-\frac{g_2^2(m_s-m_u)(m_s+m_u)}{M_\sigma^2F_K^2M_K^2}\right.\\&\left.+\frac{g_2^2(m_s-m_u)^2}{2F_K^2M_K^2M_\sigma^2}\left(1-\frac{M_\pi^2}{M_\sigma^2}\right)\right\}\\&\times\left\{-g_1g_2M_K^2+4g_2^2(m_s+m_u)\right.\\&-2(m_s-m_u)g_2^2\frac{M_K^2}{M_\sigma^2}-2(m_s-m_u)g_2^2\\&\left.\times\left(1-\frac{M_\pi^2}{M_\sigma^2}\right)\right\}.\end{aligned} \tag{D2}$$

[1] A. Alavi-Harati *et al.*, Phys. Rev. Lett. **83**, 22 (1999).
[2] M. S. Sozzi, NA48 experiment at CERN, talk given at Kaon '99 (1999).
[3] A. I. Vainstein, V. I. Zakharov, and M. A. Shifman, Sov. Phys. JETP **45**, 670 (1977) [Zh. Eksp. Teor. Fiz. **45**, 1275 (1977)].
[4] J. Bijnens and M. B. Wise, Phys. Lett. **137B**, 245 (1984).
[5] J. M. Flynn and L. Randall, Phys. Lett. B **224**, 221 (1989).
[6] C. Dib, I. Dunietz, and F. J. Gilman, Phys. Lett. B **218**, 487 (1989); Phys. Rev. D **39**, 2639 (1989).
[7] Y. Y. Keum, U. Nierste, and A. I. Sanda, Phys. Lett. B **457**, 157 (1999).
[8] E. P. Shabalin, Yad. Fiz. **48**, 272 (1988) [Sov. J. Nucl. Phys. **48**, 172 (1988)].
[9] T. Morozumi, C. S. Lim, and A. I. Sanda, Phys. Rev. Lett. **65**, 404 (1990).
[10] M. Harada, F. Sannino, and J. Schechter, Phys. Rev. D **54**, 1991 (1996); Phys. Rev. Lett. **78**, 1603 (1997).
[11] N. A. Törnqvist and M. Roos, Phys. Rev. Lett. **76**, 1575 (1996).
[12] S. Ishida, M. Y. Ishida, H. Takahashi, T. Ishida, K. Takamatsu, and T. Tsuru, Prog. Theor. Phys. **95**, 745 (1996).
[13] D. Morgan and M. Pennington, Phys. Rev. D **48**, 1185 (1993).
[14] G. Janssen, B. C. Pearce, K. Holinde, and J. Speth, Phys. Rev. D **52**, 2690 (1995).
[15] Particle Data Group, C. Caso *et al.*, Eur. Phys. J. C **3**, 1 (1998), p. 363.
[16] G. Ecker, J. Gasser, A. Pich, and E. De Rafael, Nucl. Phys. **B321**, 311 (1989).
[17] G. Ecker, J. Kambor, and D. Wyler, Nucl. Phys. **B394**, 101 (1993).
[18] G. Buchalla, A. J. Buras, and M. E. Lautenbacher, Rev. Mod. Phys. **68**, 1125 (1996).
[19] A. J. Buras, M. Jamin, and M. E. Lautenbacher, Nucl. Phys. **B408**, 209 (1993).
[20] G. Buchalla, A. J. Buras, and K. Harlander, Nucl. Phys. **B337**, 313 (1989).
[21] R. S. Chivukula, J. M. Flynn, and H. Georgi, Phys. Lett. B **171**, 453 (1986); A. J. Buras and J.-M. Gerard, *ibid.* **192**, 156 (1987).
[22] P. Colangelo, F. De Fazio, G. Nardulli, and N. Paver, Phys. Lett. B **408**, 340 (1997); M. Jamin, Nucl. Phys. B (Proc. Suppl.) **64**, 250 (1998); C. A. Dominguez, L. Pirovano, and K. Schilcher, Phys. Lett. B **425**, 193 (1998); K. Maltman, *ibid.* **462**, 195 (1999); S. Narison, hep-ph/9905264; A. Pich and J. Prades, J. High Energy Phys. **10**, 004 (1999).
[23] C. R. Allton *et al.*, Nucl. Phys. **B431**, 667 (1994); R. Gupta and T. Bhattacharya, Phys. Rev. D **55**, 7203 (1997); B. J. Gough *et al.*, Phys. Rev. Lett. **79**, 1622 (1997); SESAM Collaboration, N. Eicker *et al.*, Phys. Lett. B **407**, 290 (1997); Phys. Rev. D **59**, 014509 (1999); A. Cucchieri *et al.*, Phys. Lett. B **422**, 212 (1998); M. Gockeler *et al.*, Phys. Rev. D **57**, 5562 (1998); V. Gimenez *et al.*, Nucl. Phys. **B540**, 472 (1999); D. Becirevic *et al.*, Phys. Lett. B **444**, 401 (1998); S. Aoki *et al.*, Phys. Rev. Lett. **82**, 4392 (1999); S. Aoki *et al.*, *ibid.* **84**, 238 (2000); T. Blum, A. Soni, and M. Wingate, Phys. Rev. D **60**, 114507 (1999).
[24] W. A. Bardeen, A. J. Buras, and J.-M. Gérard, Phys. Lett. B **180**, 133 (1986).
[25] W. A. Bardeen, A. J. Buras, and J.-M. Gérard, Phys. Lett. B **192**, 138 (1987).
[26] A. J. Buras, in *CP Violation*, edited by C. Jarlskog (World

Scientific, Singapore, 1989), p. 575.
[27] CHPT corrections up to $O(p^4)$ in the chiral quark model have been discussed in S. Bertolini, J. O. Eeg, M. Fabbrichesi, and E. I. Lashin, Nucl. Phys. **B514**, 63 (1998); **B514**, 93 (1998).
[28] T. Hambye, G. O. Kohler, and P. H. Soldan, Eur. Phys. J. C **10**, 271 (1999).
[29] T. Hambye, G. O. Kohler, E. A. Paschos, P. H. Soldan, and W. A. Bardeen, Phys. Rev. D **58**, 014017 (1998).